JAEA-Technology
2007-062

JAEA-Technology

Detail Design of Microfission Chamber for Fusion Power Diagnostic on ITER

Masao ISHIKAWA, Takashi KONDOH, Atsuro HAYAKAWA*
Takeo NISHITANI and Yoshinori KUSAMA

ITER Diagnostics Group
Fusion Research and Development Directorate

December 2007
Japan Atomic Energy Agency
日本原子力研究開発機構

〒319-1195　茨城県那珂郡東海村白方白根 2 番地 4
日本原子力研究開発機構　研究技術情報部　研究技術情報課
電話 029-282-6387, Fax 029-282-5920

*〒319-1195　茨城県那珂郡東海村白方白根 2 番地 4　日本原子力研究開発機構内

JAEA-Technology 2007-062

Detail Design of Microfission Chamber for Fusion Power Diagnostic on ITER

Masao ISHIKAWA, Takashi KONDOH, Atsuro HAYAKAWA*, Takeo NISHITANI and Yoshinori KUSAMA

ITER Project Unit
Fusion Research and Development Directorate
Japan Atomic Energy Agency
Naka-shi, Ibaraki-ken

(Received October 17, 2007)

The microfission chambers (MFCs) provide time-resolved measurements of the global neutron source strength and fusion power from ITER. In the previous work, the MFC for low power operations (measurement range : fusion power of 100 W – 1 kW) has been designed and developed together with the MFC for high power operation (measurement range : fusion power of 1 kW – 1 GW). Combination of two types of the MFC almost covers the target measurement requirements of ITER. Signals from the MFCs are transferred by double coaxial mineral Insulated (MI) cables. The MFCs will be installed in the vacuum vessel, so that the MI cables should be placed in the vacuum vessel. In this design work, the placing route of the MI cables from the installation position of the MFC to the feed-through in the upper port is designed. As far placing of the MI cable, since the MI cable is filled with Ar gas at 14.6 atom, the double pipe structure, in which the outer pipe covers the MI cable, is going to be adopted in order to prevent the gas leak into the vacuum vessel. The exhaust system of the double pipe is also designed for detection and exhaust of the leaked Ar gas. Further, we design that copper flanges with 7 mm width for heat conductance will be installed between the MI cable and the outer pipe at interval of 300 mm, in order that the maximum temperature of the MI cable due to temperature rise by the nuclear heating doesn't exceed the operating temperature (400 °C) of the MI cable in a light-water reactor. As a result, it is found that the temperature of the MI cable can be suppressed less than 340 °C.

Keywords: Neutron Monitor, Microfission Chamber, MI Cable, ITER, Fusion Power, Neutron Source Strength

---

* Toshiba Corp.

ITERにおける核融合出力診断用 マイクロフィッションチェンバーの詳細設計

日本原子力研究開発機構
核融合研究開発部門 ITERプロジェクトユニット
石川　正男、近藤　貴、早川　敦郎*、西谷　健夫、草間　義紀

（2007年10月17日受理）

マイクロフィッションチャンバーは、ITERにおける全中性子発生量および核融合出力の時間分解測定を与える。これまで、低出力用のマイクロフィッションチャンバー（測定範囲：1 kW – 100 kWの核融合出力）の設計・開発を高出力用のマイクロフィッションチャンバー（測定範囲：100 kW – 1 GWの核融合出力）とともに行ってきた。これらの検出器を組み合わせることで、ITERで目標とされる計測要求をほぼ満たすことができる。マイクロフィッションチェンバーは真空容器内に取り付けられるため、信号出力・電力供給として用いられる2重同軸Mineral Insulated（MI）ケーブルも真空容器上に敷設する必要がある。今回は、マイクロフィッションチャンバー設置位置から上部ポートのフィードスルーまでのMIケーブルの真空容器内における敷設ルートの設計を行った。また、MIケーブルには14.6気圧のArガスが封入されているが、Arガスの真空容器内へのリークを防ぐために、敷設に際してはMIケーブルを外管で包む二重配管を採用した。この配管にはArガスがリークした場合に検知、排気するための排気装置を付ける。さらに、核発熱による温度上昇によってMIケーブルの最高温度が軽水炉でのMIケーブルの使用温度（400℃）を超えないように、MIケーブルと外管の間に300mmごとに熱伝導のための7mm幅の銅フランジを入れる設計を行った。その結果、MIケーブルの温度は、340℃以下に抑えることができることがわかった。

*（株）東芝

Contents

目　次

1. Introduction

1.1 Design requirements

The microfission chamber (MFC) provides time-resolved measurements of the global neutron source strength and fusion power. The target measurement specifications for the MFC (ITER WBS Number: 5.5.B.03) are listed in Table 1.1-1 In the previous work, the MFC for low power operation (measurement range: fusion power of 1 kW – 100 kW) [1] was designed together with the MFC for high power operation (measurement range : fusion power of 100 kW – 1 GW) [2 – 6]. Combination of two types of the MFC almost covers the target measurement requirements.

1.2 Objectives

Signals from the MFC are transferred by a double coaxial mineral insulated (MI) cable. The MFCs will be installed in vacuum vessel, so that MI cables should be also placed in the vacuum vessel. In this design work, the placing route of the MI cable in the vacuum vessel will be designed. The MI cable is filled with Ar gas at 14.6 atm. So, double pipe structure, in which the outer pipe covers the MI cable will be designed to prevent the gas leak into the vacuum vessel. The exhaust system of the double pipe will be also designed. The maximum temperature of the MI cable due to nuclear heating should be considered.

In this report, design description of the MFCs for low and high power operation, which were designed in the previous works, is described in Chap.2. In the last section in Chap.2, a new design work to develop the MFC is also presented. Chapter 3 reports the design work of placing of the MI cable in the vacuum vessel. The maximum temperature of the MI cable due to the nuclear heating is also evaluated. The design work of external connection of the MI cable at the feed-through part and the exhaust system of the MI cable is reported in Chap.4. Finally, the summary of this design work and future work are presented in Chap.5.

2. Conceptual Design Description of the Microfission Chamber (MFC)

In this chapter, the conceptual design of the MFC in the previous work is described. But, a new design work to develop the MFC is presented in Sec.2.5

2.1 MFC

(a) MFC for high power operation

A MFC is a pencil size gas counter with fissile material inside, which was developed as in-core monitor of the fission reactor. Figure 2.1-1 (a) shows the schematic view of the typical MFC designed for ITER. In this MFC, UO_2 is coated in the outer cylindrical electrode with a coating density of 0.6 mg/cm^2. The active length is 76 mm, and the total amount of UO_2 is 12 mg. Because the enrichment of ^{235}U is 90%, the total amount of ^{235}U is about 10 mg. This MFC is filled with 95% Ar and 5% N_2 gas at 14.6 atm. The housing material is stainless steel 316 L, and the electric insulator is alumina (Al_2O_3). Fig.2.1-1 (b) shows a full body drawing of the fabricated MFC and the double coaxial mineral insulated (MI) cable, which is welded directly to the MFC. The cable uses SiO_2 as an electric insulator with a packing density of 30%, and it is filled with Ar at 14.6 atm. The center conductor is insulated not only with the SiO_2 insulator but also the Ar gas. In the case of cracking at the electric insulator in the MFC due to swelling, the Ar gas in the MI cable will prevent the lack of the gas pressure in the MFC.

Wide dynamic range of 10^7 in a single fission chamber has been demonstrated in the JT-60U neutron monitor system [7] with both counting mode and Campbelling mode (mean square voltage) [8]. The linearity is calibrated using a fission reactor. Because the pulse width of the fission chamber output is about 100 ns, the maximum pulse counting rate is about 10^6 counts/s due to pulse pile-up. The Campbelling mode is available for an equivalent counting rate larger than 10^5 counts/s. One decade overlap was confirmed for pulse counting and Campbelling modes in the case of the JT-60U neutron monitor. As a result, an expected dynamic range of MFC with 10mg ^{235}U covers 100 W through 1 GW of ITER operation power as shown in Fig.2-1-2. However, the statistical error of the pulse counting less than 10^5 counts/s doesn't satisfy the required accuracy of ITER. So, it is found that the realistic dynamic range with the statistical error less than 10 % for 1 ms sampling time is 100 kW – 1 GW of fusion power.

(b) MFC for low power operation

The dynamic range of the MFC described above could not cover power operations less than 100 kW and DD operation. The MFC for low power operation was designed [1].

About 750 mg of ^{235}U is needed for the MFC in order to measure neutron flux within the required accuracy for the low power operations (1 kW – 100 kW). If 90% enriched Uranium is used, 833 mg of U is required to obtain 750mg of ^{235}U. So 950mg of UO_2 is needed. Maximum thickness of UO_2 on the electrode is 1 mg/cm^2. Therefore, the required electrode area is 950 cm^2.

The MFC for low power operations consists of bundle of MFC elements, taking into account for installing it in a narrow space between the vacuum vessel and the blanket module. Fig.2.1-3 shows the schematic view of the MFC element for low power operations. The element is based on the MFC for high power operation with outer diameter of 6 mm. The sensitive area of the element is 24.6 cm^2. In order to keep the total sensitive area of 950 cm^2, 39 elements is necessary. Schematic view of the MFC for low power operation consisting of 39 MFC elements is shown in Fig.2.1-4.

Dynamic range of the MFC for low power operations is shown in Fig.2.1-5. Combining pulse counting mode and Campbelling mode and keeping the statistics error of the counting mode to be less than 10 %, total dynamic range is evaluated to be 1 kW – 10 MW for 1ms sampling time.

By combining the MFCs for high power operations and for low power operations, the target measurement requirement as shown in Tab.1.1-1 is almost covered. Further, for longer sampling time such as 10 ms at the lower fusion power, we can extend the measurement limit to fusion power of 100 W. The performance of these MFCs is listed in Tab.2.1-1

2.2 Installation position

The MFC will be installed in the vacuum vessel. However, since streamed neutrons are dominant in the gap between adjacent blanket modules, the change of the gap width due to a thermal expansion or mechanical movements would change the neutron flux. Thus, the location behind the blanket module is adopted to install the MFCs.

In order to find the poloidally suitable position of MFCs, neutron transport calculations by the Monte Carlo method was performed with the Monte Carlo code for neutron and photon transport (MCNP) Version 4B [9] and a neuron cross-section set based on JENDL-3.2 [10]. Changes of the detection efficiency for the changes of the horizontal, vertical plasma positions and the peaking factor of the neutron source profile were calculated. As a result, position at the blankets #11 and #16 turned out almost insensitive to the changes in the horizontal plasma position and the peaking factor. As for the changes in the vertical plasma position, the average outputs of the chambers at #11 and #16 cancel out each other. The proposed arrangement of the MFC on ITER is shown in Fig.2.2-1. As for toroidal arrangements, two directions were selected for redundancy.

At each installation position, a set of the MFCs (two MFCs and a dummy chamber, which has the same structure as the MFC, except no uranium coating on the electrode) will be installed for the MFC for high power operations. The reason why two MFCs are installed at the same position is because one MFC must be operated at least even if another one is broken. A dummy chamber is also installed for the gamma-ray effect compensation.

2.3 Lifetime

A lifetime of the MFC is determined by the change of the sensitivity of the chamber due to the burn-up of the fissile material. The isotope ^{235}U burns mainly through fission and neutron capture reactions. For the MFC position the behind the blanket module (typically #11), the burn-up of ^{235}U atoms is dominated by the fission reaction, because the fission cross section is about 10^2 times larger than the capture one. Since the burn-up rate was evaluated to be 2.7×10^{-11} s^{-1}, the sensitivity change was only 0.1% behind the blanket module for the ITER lifetime, which is equivalent to 0.5 GW operation for year. Thus, the ^{235}U chambers can be used without replacement during the ITER lifetime.

2.4 Test of the MFC [11]

The MFC for high power operations was tested for the JT-60U operation under magnetic field of about 2 T. The MFC was covered with the Polyethylene block ($220 \times 100 \times 45$ mm^3) as a moderator and an electric insulator. It had been installed between the vacuum vessel and toroidal coils as shown in Fig.2.4-1. The performance of neutron measurements of the MFC was compared with JT-60U neutron monitor [7] (^{235}U fission chamber), which was absolutely calibrated using the ^{252}Cf neutron source. The influence of the magnetic field up to 2 T has not been observed. Figure 2.4-2 shows the linearity of the MFC for the neutron monitor. The MFC has the excellent linearity over 3 decades of neutron flux range. The standard deviation between the neutron yield obtained by these detectors was 3 % including the stability of the Campbell electronics.

2.5 Extension of lifetime of the electric insulator by using Si_3N_4 insulator

Since the electric insulator using alumina (Al_2O_3) could be cracked due to swelling, the MI cable is filled with Ar gas at the same pressure as the MFC to prevent the lack of the pressure of Ar gas in the MFC. Recently, an electric insulator using Si_3N_4 has been developed for long lifetime operation of the MFC used in a fission reactor [12-14]. Si_3N_4 has the property of low swelling (about half of the alumina) and excellent electrical isolation. It was evaluated that fracture life of the electric insulator expands more than 25 years by using Si_3N_4. In the fission reactor, neutron irradiation to the electric insulator is ~ 1.5×10^{25} n/m^2 per one year. So neutron fluence until Si_3N_4 insulator Q_{Si3N4} is cracked is evaluated to be more than 3.5×10^{26} n/m^2. On the other hand, neutron fluence at the vacuum vessel during DT operation and wall loading are evaluated to be 0.3 MWa/2 and 0.56 MW/m2, respectively (ITER Project Integration Document). Neutron flux is also estimated to be 2.4×10^{14} n/cm^2/s. Taking into account that neutron flux is attenuated about 2 order due to the blanket module, neutron fluence to the MFC installed behind the blanket module during DT operation, Q_{MFC} is given by

$$Q_{MFC} = 0.3/0.56 \text{ x } 3600\text{x}24\text{x}365 \text{ x } 2.4\text{x}10^{14} \text{ x } 10^{4} \text{ x}10^{-2} \sim 4\text{x}10^{23} \text{ n/m}^2.$$

Therefore, $Q_{Si3N4} >> Q_{MFC}$. This indicates that the Si_3N_4 electric insulator can survive during the ITER lifetime. However, since there is a possibility that the electric insulator could be broken due to the electro-magnetic force by disruption, it is necessary that the MI cable is filled with Ar gas. Effect of the electro-magnetic force on the electrical insulator should be evaluated experimentally in future work.

3 Conceptual Design of Placing of the MI Cable [15, 16]

3.1 Structure of the MI cable in the vacuum vessel

The MI cable is filled with Ar gas at 14.6 atm to prevent the lack of the gas pressure in the MFC in the case of cracking at the electrical insulator. There is a possibility that Ar gas in the MI cable is leaked into the vacuum vessel when the MI cable is ruptured. Since the ITER regulation requires that allocated integrated global leak rate into the primary vacuum boundary is less than 10^{-8} Pam^3/s for diagnostics (ITER Vacuum Design Handbook 2234LX), the leak of Ar gas from the MI cable must be prevented. Therefore, we design a double pipe, in which the MI cable ($\phi \sim$ 6mm) is covered with an outer pipe ($\phi \sim$ 13.2 mm, SUS), as shown in Fig.3.1-1. The exhaust system for leaked Ar gas or outgas from the MI cable is installed in this double pipe. The exhaust system is described in Chap.4. The minimum curvature of the double pipe is R = 100 mm.

3.2 Design of placing of the MI cable

The placing route of the MI cable covered with the outer pipe have been investigated and designed. Figure 3.2-1 shows the whole placing route of the MI cable on the vacuum vessel with the water manifold. Since two MFCs and one dummy chamber will be installed at behind the blanket #11 and #16 for high power operation, 3 MI cables are placed from each installation position to the feed-through part in the upper port on the vacuum vessel.

3.2.1 Placing on the vacuum vessel

The clearance between the vacuum vessel and the blanket module is about 25mm as shown in Fig.3.2-2. Further, the clearance could become narrower due to thermal expansion of a cooling tube, which pass trough a witch dug in the blanket module as shown in Fig.3.2-3. Thus, the MI cable needs to be placed in the narrow space between the vacuum vessel and the blanket module. The suitable placing route is designed.

(a) Lower MFC

Figure 3.2-4 shows the placing route of the MI cable for the MFC installed at behind the blanket module #16 (lower-MFC). The MI cables are placed on the vacuum vessel by skirting stub keys as shown in Fig.3.2-5. After MI cables pass through under the fillers as shown in Fig.3.2-4, those go into the upper port. Figures 3.2-6 and 3.2-7 show the cross-sectional views of Figs.3.2-4 and 3.2-5, respectively. The clearance between the MI cables and the blanket module or the filler is tight, but it is secured larger than 10 mm.

(b) Upper MFC

Figure 3.2-8 shows the placing route of the MI cable for the MFC installed at behind the blanket #11 (upper-MFC). The MI cables are placed horizontally from the detector. After the MI cables are bended, those go up left side of the upper port.

3.2.2 Placing at the upper port

The design of MI cable placing near the upper port is shown in Fig.3.2-9. The MI cables for the lower-MFC place on the right sidewall and goes up in the upper port. The clearance for placing in the upper port is tight, too. The narrowest space is between the cooling pipes and the sidewall of the upper port as shown in Fig.3.2-10. The MI cables for the upper-MFC are placed on the left sidewall and also goes up in the upper port as shown in Fig.3.2-8. These MI cables for the lower- and the upper-MFC are lumped together at upper part in the upper port and go to the feed-through.

3.3 Overall length of the MI cable

Overall length of the MI cables for the lower- and the upper-MFC are 4784.3 mm, and 12690.7 mm, respectively. Figure 3.3-1 shows whole placing route of MI cables from each MFC position to the feed-through, together with the ITER vacuum vessel including the water manifold. Figures 3.3-2 and 3.3-3 show the bending point of the MI cables. The curvature (R) and the arc length of curve at each bending point are listed in Tab.3.3-1. The minimum curvature is R = 120 mm, which is larger than the minimum allowed curvature of the double pile that the MI cable covers with the outer pipe.

3.4 Adjustment of MI cable length

Since the MI cable filled with Ar gas is welded with the MFC, whole structures, which consist of the MFC, the MI cable and the connectors, must be made in a factory. On the other hand, dimension error of the vacuum vessel could be observed. Since the MI cable cannot be cut at the ITER site, length adjustment of the MI cable is necessary. We design that length of the MI cable is adjusted by changing straight portion to S-shaped curve. The S-shaped curve is made by combining two circular arcs with R = 500 mm, θ = 30° as shown in Fig.3.4-1. The curve can absorb length in 6 mm per 500 mm of the straight portion. It is possible to adjust 24 mm and 66 mm in length of MI cable of the upper-MFC (total length 4784.3 mm) and of the lower-MFC (total length 12690.7 mm), respectively. Also, Length of the MI cable can be adjusted +/- 8mm at the feed-through by using bellows.

3.5 Evaluation of the maximum temperature of the MI cable

Temperature of the MI cable is rose due to the nuclear heating. So, cooling of the MI cable is necessary in order that the maximum temperature of the MI cable does not exceed the operating temperature in the light-water nuclear reactor (400 c). However, though the outer pipe is contacted with the vacuum vessel, which is cooled with coolant water, the MI cable is not directly contacted with that. Here, necessary heat conduction between the MI cable and the outer pipe is investigated, after taking into account heat conduction between the vacuum vessel and the outer pipe. Diameter and nuclear heating for the fusion power operation of 0.5 GW of the MI cable and the outer pipe is listed in Tab.3.5-1, respectively. Here, heat conduction of the MI cable to longitudinal direction in not considered. Also, it is assumed that temperature of the vacuum vessel is kept at 150 C° by water cooled tubes.

(a) Heat conduction between the vacuum vessel and the outer pipe

The outer pipe is contacted with the VV at one point as shown in Fig.3.1-1. Assuming that the contact area is 1 % of the perimeter of the outer pipe, the contact length per unit length to longitudinal direction is 4.14×10^{-4} m. If heat conductivity of the contact part is ~ 500 W/m^2K, heat conductivity per unit length, a_1 is given 0.207 W/mK. Here, assuming that nuclear heating Q_1 balance with heat conduction between the vacuum vessel and the outer pipe, temperature rise of the outer pipe

(ΔT_1) of the outer pipe for the vacuum vessel is given by

$$Q_1 = a_1 \times \Delta T_1$$

Substituting the value of Q_1 and a_1 to above equation,

$$\Delta T_1 = 13.8.$$

Since the temperature of the vacuum vessel is 150 °C, temperature of the outer pipe is evaluated as ~ 163.8 °C

(b) Heat conduction between the MI cable and the outer pipe

Since the MI cable is contacted with the outer pipe only due to the MI cable's own weight without any procedure as shown in Fig.3.1-1, the heat conductance is not sufficient. So, we design that copper flanges are inserted between the MI cable and the outer pipe in order to ensure the heat contact as shown in Fig.3.5-1. Here, the necessary width of the flange per unit length w_f is evaluated in order that the maximum temperature of the MI cable doesn't exceed the operating temperature in the fission reactor (400 °C). Setting that the effective area for heat conduction is half of the flange to ensure the aperture for exhaust of leaked gas, arc length of the contact part of the MI cable is 3π mm because the diameter is 6 mm. Also, assuming that the nuclear heating balance with heat conduction between the MI cable and the outer pipe via the flange, the nuclear heating of the MI cable Q_2 is given by

$$Q_2 = a_2 \times \Delta T_2$$

where a_2 is heat conductivity per unit length (W/mK) given by

$$a_2 = 500\ (\mathrm{W/m^2K}) \times 3\pi \times w_f,$$

and ΔT_2 is the temperature rise of the contact part. Here, allowable temperature rise, ΔT_2 is set to be 50 K in order that the maximum temperature of the MI cable between the contact parts with the flanges is sufficiently below 400°C. Then, the necessary width of the flange per unit length, w_f is evaluated to be ~ 0.0023. So, we design that the copper flange with width of 7 mm is installed at interval of 300 mm. By these procedure, the temperature of the MI cable at the contact part with the outer pipe can be suppressed less than 214 °C. On the other hand, temperature of the MI cable increase as the distance from position contacted with the flange increases. Then, the maximum temperature of the MI cable should be evaluated. Here, heat conduction of 1-dimension to longitudinal direction (x-direction) is considered. Setting the contact position as x = 0, total nuclear heating Q*(x) at the position x is given by

$$Q^*(x) = Q \times x.$$

Assuming that heat conduction of the MI cable to longitudinal direction balances with the nuclear heating,

$$K\ dT = Q^*(x)\ dt,$$

where K is the heat conductivity per unit length to longitudinal direction, which given by k × s and k is the heat conductivity per unit area and s is the cross sectional area of the MI cable. So,

$$\Delta T = 1/2 \times Q/ (k \times s) \times x^2.$$

Since the flanges are put at interval of 0.3 m, x at the maximum temperature is given 0.15 m. Then, substituting that Q = 5.06 (W/m), k = 16 (W/mk) s = 2.8×10^{-3} (m^2) and x = 0.15 (m), the maximum temperature rise is estimated ΔT_{max} = ~126 K. Since the temperature of the contact position between the outer pipe and the MI cable is 214 °C, the maximum temperature of the MI cable is evaluated to be

$$T_{max} \sim 340\ (°C).$$

Thus, it is found that the MI cable inside the double pipe can be operated in the ITER operating environment, by inserting the copper flange of 7 mm width at interval of 300 mm.

3.6 Schedule of MI cable placing

It is considered that placing of MI cable is possible at two different timings.

A: During fabrication of vacuum vessel sector

B: After installation of whole vacuum vessel

In the case of A, it has no big problems for placing the MI cable because it can be installed from a section of the sector. On the other hand, in the case of B, the MI cable should be placed before installation of cooling tubes (especially, water manifold), because MI cable is placed under the cooling tubes. A is better than B as for cabling the MI cable. However, since the MFC includes the nuclear material (UO_2), It should be negotiated with ITER organization for the schedule and the way of the transport of nuclear material.

4. Design of External Connection of the MI Cable

4.1 Constructive concept of external connection of the MI cable

As far placing of the MI cable in the vacuum vessel, the double pipe that the outer pipe covers the MI cable is adopted to prevent Ar gas leak into the vacuum vessel. On the other hand, emission of gas absorbed to the MI cable (outgas) at the connection part and the terminal part became an issue for the magnetic measurement, recently [17] In order to solve this issue, it has been investigated that outgas is exhausted by making pinholes in the MI cable. However, since the MI cable of the MFC is filled with Ar gas, it cannot be made a pinhole in the MI cable. Therefore, the double pipe structure is also needed for not only Ar gas leak but also the outgas from the MI cable. It is necessary that leaked Ar gas from the MI cable can be detected and exhausted for the long time operation of the MFC. So, we design the exhaust system for the double pipe. Figure 4.1-1 shows the constructive concept of the exhaust system of the double pipe. Leaked Ar gas is actively exhausted in the inter-space in this design by using a pump.

4.2 Structure of feed-through

External connection of MI cable at the feed-through part is designed based on the constructive concept above. Figure 4.2-1 shows the detail structure of feed-through part. The MI cable is connected with the soft cable out of the vacuum vessel via the connector attached to the flange. The exhaust tube and the exhaust valve are also attached to the flange. The MI cable length can be adjusted by using the bellows installed at the feed-through part as described in Sec.3.4. +/- 8mm adjustable bellows is used in this design. Figure 4.2-2 shows schematic view around the feed-through together with the pre-amplifier and the main amplifier. The soft cable from the feed-through is connected with the pre-amplifier. In order to suppress noise effects, the pre-amplifier should be placed in such way the distance between feed-through and the pre-amplifier is as short as possible. After connecting to the main-amplifier, electric signal is transformed to optical signal and connected to the data acquisition system in the diagnostic room.

4.3 Evaluation of Ar gas leak and outgas from the MI cable

Ar gas leak and outgas emission from the MI cable in this double pipe is evaluated. Assuming the double pipe as a long concentric cylinder, conductance C for the concentric cylinder is given by

$$C = 121 \times K \times (d_1-d_2)^2 \times (d_1+d_2)/L \ [18],$$

where, d_1, d_2 are the inner diameter of the outer pipe, the outer diameter of the MI cable, respectively, and L is the length of the concentric cylinder. From table 3.5-1 and Section 3.3,

$$d_1 = 11.2 \times 10^{-3} \text{ m},$$
$$d_2 = 6.0 \times 10^{-3} \text{ m},$$
$$L \sim 13 \text{ m}.$$

Also, K is the correction coefficient decided from the relation between d_1 and d_2 and is given by

$$K = 1.2.$$

Then, the conductance is estimated to be

$$C = 4.3 \times 10^{-6} \text{ m}^3/\text{s}.$$

On the other hand, gas emission velocity per unit area from a concentric cylinder (electrolytically-polished SUS) is measured to be 2.2×10^{-8} Pam^3/s/m^2 as presented in ref.19. Since the total area inside the double pipe is given by

$$S = p \times (d_1 + d_2) \times L$$
$$\sim 1.7\ m^2,$$

the gas emission velocity inside the double pipe due to outgass, $Q_{outgass}$ is evaluated to be

$$Q_{outgass} = 3.74 \times 10^{-8}\ Pam^3/s.$$

Then, The balance pressure of this exhaust system is dominated by the low conductance even if the pump with large exhaust velocity is used and is given by

$$P = Q_{outgass} / C$$
$$\sim 10^{-2}\ Pa.$$

Here, the Ar gas leak from the MI cable is considered. If the MI cable is ruptured, gas emission velocity of leaked Ar gas is evaluated to be ~ $1 \times 10^{-6}\ Pam^3/s$. In this case, since the balance pressure of the leaked Ar gas is 1 order higher than outgas, the Ar leak can be detected. On the other hand, if the rupture area is about 100 mm in diameter, gas emission velocity of leaked Ar gas is evaluated to be ~ $1 \times 10\text{-}^{9}\ Pam^3/s$. In this case, since the balance pressure is about 2 order lower than outgass, the change of pressure cannot be observed. Therefore, a mass analyzer to detect the Ar leak is necessary.

5. Summary and Future work

5.1 Summary

The MFCs will be installed at the two different poroidal sections (behind blanket modules at upper outboard and lower outboard) in vacuum vessel in order to measure neutron flux without the effect of the changes in the plasma position and neutron source profile. MI cables of the MFC should be also placed in the vacuum vessel. In this design work, the placing route of the MI cable from each MFC position to the feed-through in the upper port will be designed. Since the MI cable is filled with Ar gas at 14.6 atom, the double pipe structure that the outer pipe covers the MI cable will be designed in order to prevent the gas leak into the vacuum vessel. The whole lengths of the double pipes of the upper and the lower MFC are 4784.3 mm and 12690.7 mm, respectively. The minimum curvature is R = 120 m. The maximum temperature of the MI cable due to the nuclear heating was evaluated. It is found that the temperature of the MI cable might be less than 340 °C, which is lower than the operation temperature of the MI cable in a fission reactor, by installing copper flanges with 7 mm width between the MI cable and the outer pipe at interval of 300 mm for heat conductance. This indicates that the MI cable inside the double pipe can be operated in the ITER operating environment. The external connection of the double pipe is also designed. In this design, leaked Ar gas from the MI cable is exhausted to the inter-space by using the exhaust tube and valve connected with the flange with the connector at the feed-through part.

5.2 Future work

In present design work, the placing route of the double pipe on the vacuum vessel was designed. However, it should be confirmed that the space between the double pipe and other equipment (the cooling pipes, the water manifold, etc) is sufficient or not. The way of placing of the double pipe in the narrow space should be investigated in future design work. Detail design work of the exhaust system of the double pipe is one of future design work. On the other hand, the MFC and the double pipe are shocked from the electro-magnetic force due to disruption. Since the test of the mechanical shock had been performed only for the MFC, effect of the electro-magnetic force on the electrical insulator using Si_3N_4 of the MFC and the double pipe should be evaluated experimentally. The cause of the electrical noise on the MI cable should be also identified and resolved, which was observed in the performance test of the MFC was in JT-60U.

Acknowledgments

The authors appreciate Dr. S. Yamamoto for his pioneering work on the microfission chambers in ITER CDA.

References

[1] Nishitani, T,. et al., “Design of Micro-Fission Chambers for ITER Low Power Operations”, Japan Atomic Energy Research Institute, JAERI-Tech 2005-047 (2005).
[2] Nishitani, T., et al., “Design of ITER Neutron Monitor using Micro Fission Chambers”, Japan Atomic Energy Research Institute, JAERI-Research 98-049 (1998).
[3] Nishitani, T., et al., “Neutron monitor using microfission chambers for the International Thermonuclear Experimental Reactor”, Rev. Sci. Instrum. **70** 1141 (1998).
[4] Nishitani, et al., “Design of in-vessel neutron monitor using micro fission chambers”, Japan Atomic Energy Research Institute, JAERI-Tech 2001-066 (2005).
[5] Yamauchi, M., “Performance Test of Micro-fission Chambers for In-vessel Neutron Monitoring of ITER”, Japan Atomic Energy Research Institute, JAERI-Tech 2002-032 (2002).
[6] Yamauchi, M., “Development of In-vessel Neutron Monitor using Micro-Fission Chambers for ITER”, Rev. Sci. Instrum. **74** 1730 (2003).
[7] Nishitani, T., et al., “Absolute calibration of the JT-60U neutron monitors using a ^{252}Cf neutron source”, Rev. Sci. Instrum. **63**, 5270 (1992).
[8] Endo Y., et al., “A-Counting-Campbelling Neutron Measurement System and its Experimental Results by Test Reactor”, IEEE Trans. Nucl. Sci. **NS-29**, 714 (1982).
[9] Briesmeister, J.F., “MCNP – A General Monte Carlo N-Particle Transport Code, version 4B”, LA-12625-M, Version 4B, Los Alamos National Laboratory (1997).
[10] Nakagawa, T., “Japanese evaluated nuclear data library version 3 revision-2: JENDL-3.2”, J. Nucl. Sci. Technol. **32**, 1259 (1995).
[11] Hayashi, T., et al., “First measurement of time-resolved neutron yield on JT-60U using a microfission chamber”, Rev. Sci. Instrum. 75, 3575 (2004).
[12] Kawakami, S., et al, “Latest Nuclear Monitoring Instrumentation and Control System and Its Planned Application”, TOSHIBA Review **Vol1.57 No.4**, 19 (2002).
[13] Nakahasni, M., et al., “Design of Silicon Nitride and Stainless Steel joint for Airtight Seal parts”, Journal of Japan Welding Society, **21**, 374 (2004).
[14] Nakahasni, M., et al., “Tensile Strength Change of Silicon Nitride/Stainless Steel Joints during Neutron Irradiation”, Journal of Japan Welding Society, **23**, 88 (2005).
[15] Kondo, T., Ishikawa, M., et al., “Microfission Chamber” 12th Meeting of the ITPA Topical Group on Diagnostics, (Mar. 2007, Princeton, USA).
[16] Kondo, T., Ishikawa, M., et al., “Design of Microfission Chamber for ITER and Experiences of Neutron Activation System in JT-60U”, First KO-JAWorkshop on

ITER Diagnostics, (Jun. 2007 Daejeon, Korea).
[17] Vayakis, G., “Out-gassing of ITER in-vessel cabling, mitigation measures and possible tests”, N 55 RI 33 03-10-01 W 01 (2001).
[18] Vacuum Handbook, Chap 1, Sec.7, Ohmsha (2002).
[19] Vacuum Handbook, Chap 1, Sec.8, Ohmsha (2002).

Table 1.1-1
Target Measurement Requirements

Total neutron flux				
Parameter	Parameter range	Spatial res.	Time res.	Accuracy
Total neutron flux	$10^{14} – 10^{21}$ ns^{-1}	Integral	1ms	10 %
Fusion power	< 1 GW	Integral	1ms	10 %

Table 2.1-1
Performance of the MFCs for high and low power operation

	for high power operation	for low power operation
Diameter of element	14 mm	6 mm
Active length of element	76 mm	87 mm
Uranium coating density	0.6 mg/cm^2	1 mg/cm^2
Number of element	1	39
Total amount of Uranium	12 mg of UO_2	950 mg of UO_2
Ionizing gas	14.6 atm of Ar +5 % N_2	14.6 atm of Ar +5 % N_2
Range of fusion power	100kW – 1 GW	100 W – 100 kW
Time resolution	1 ms	1 ms
Accuracy	less than 10 % error	less than 10 % error

Table 3.3-1

Curvature of the MI cable at each bending point

lower-MFC

No.	R	length	degree	accumulated length
1	S	343.5		343.5
2	150	157	60	500.5
3	S	1627.8		2128.3
4	120	188.5	90	2316.8
5	S	32.75		2349.55
6	120	166.5	79	2516.05
7	S	796.5		3312.55
8	150	102.4	39	3414.95
9	S	80.5		3495.45
10	150	108.5	41	3603.95
11	S	175		3778.95
12	150	235.7	90	4014.65
13	4983	2155.8	25	6170.45
14	150	78.6	30	6249.05
15	S	72		6321.05
16	150	78.6	30	6399.65
17	150	349.9	134	6749.55
18	150	78.6	30	6828.15
19	S	72		6900.15
20	150	78.6	30	6978.75
21	4983	446.7	5	7425.45
22	2988	1182.7	23	8608.15
23	150	78.5	30	8686.65
24	S	73.6		8760.25
25	150	78.2	30	8838.45
26	2988	334.5	6	9172.95
27	150	78.5	30	9251.45
28	S	122		9373.45
29	150	73	28	9446.45
30	S	1568.6		11015.05
31	248.8	400	92	11415.05
32	S	340.4		11755.45
33	150	26.3	10	11781.75
34	S	525.1		12306.85
35	150	233.8	89	12540.65
36	S	150		12690.65

upper-MFC

No.	R	length	degree	accumulated length
A	S	343.5		343.5
B	150	157	60	500.5
C	S	1627.8		2128.3
D	120	188.5	90	2316.8
E	S	266.6		2583.4
F	150	208.1	79	2791.5
G	S	796.4		3587.9
H	150	105.9	39	3693.8
I	5597	497.1		4190.9
J	150	191.4	41	4382.3
K	S	402		4784.3

S : Straight part

Table 3.5-1
Structure of the double pipe

	Diameter (m)	thick of outer skin (mm)	Nuclear heating per unit length (W/m)
MI cable	6.0×10^{-3}	5×10^{-4}	5.06
outer pipe	1.32×10^{-2}	1×10^{-3}	2.85

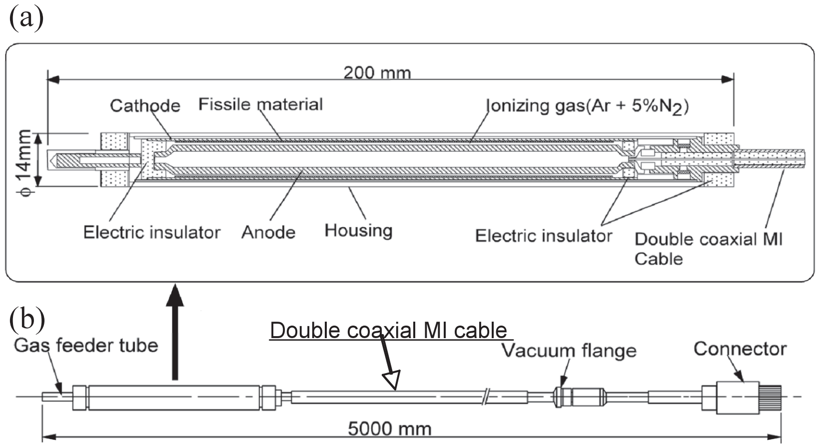

Fig.2-1-1

Schematic view of the MFC for high power operation

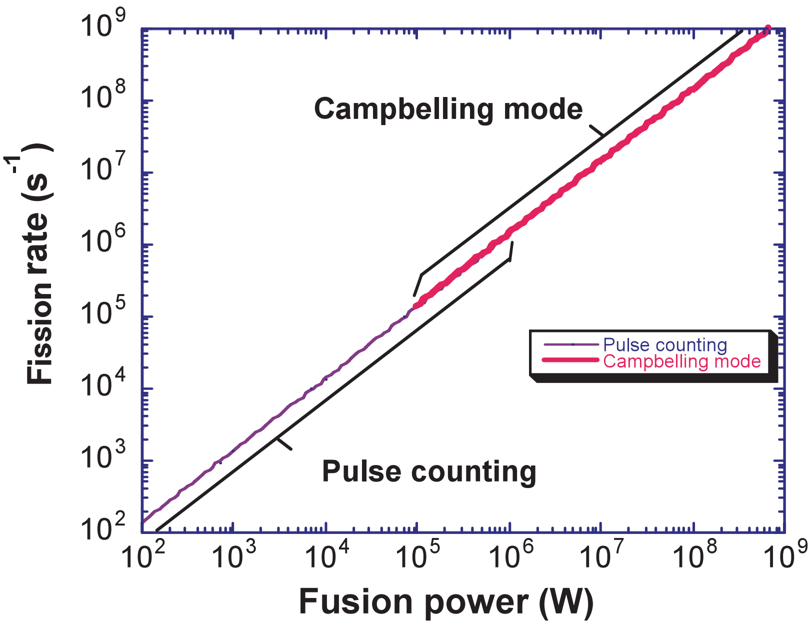

Fig.2.1-2

Dynamic range of the MFC for high power operation.

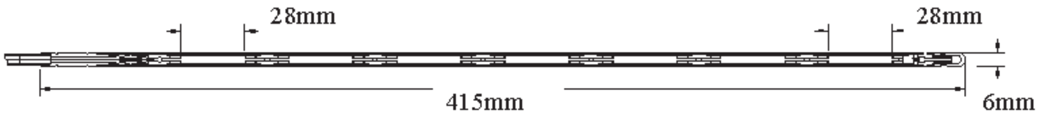

Fig.2.1-3
Schematic view of the MFC element.

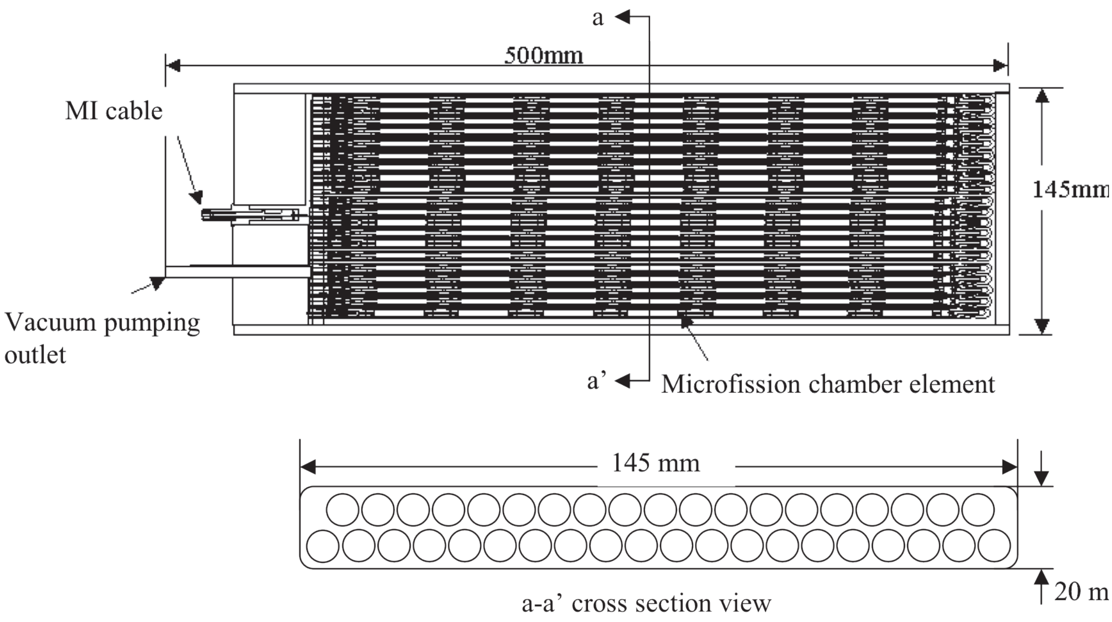

Fig.2.1-4
Schematic view of the MFC for low power operation

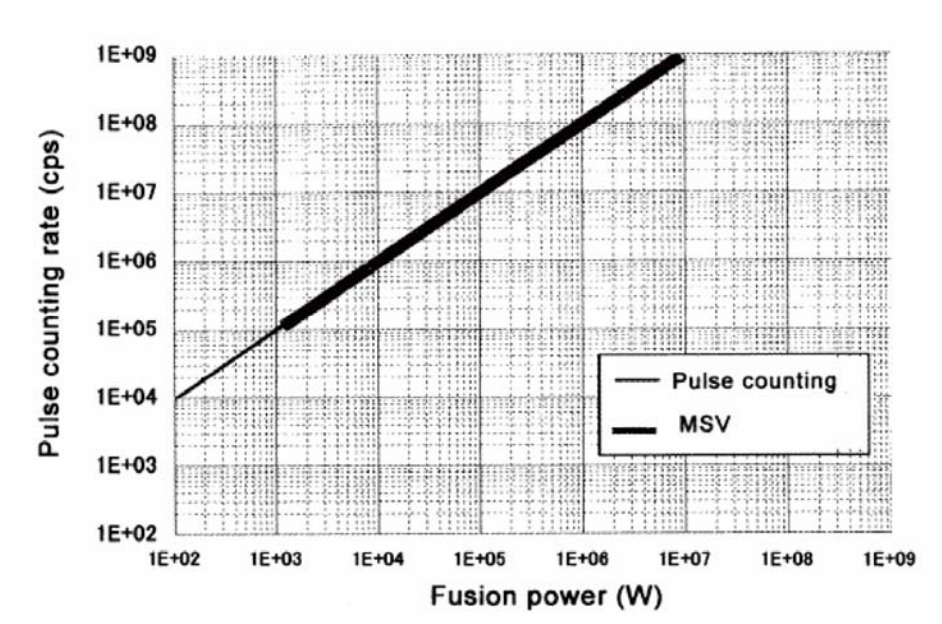

Fig.2.1-5
Dynamic range of the MFC for low power operation

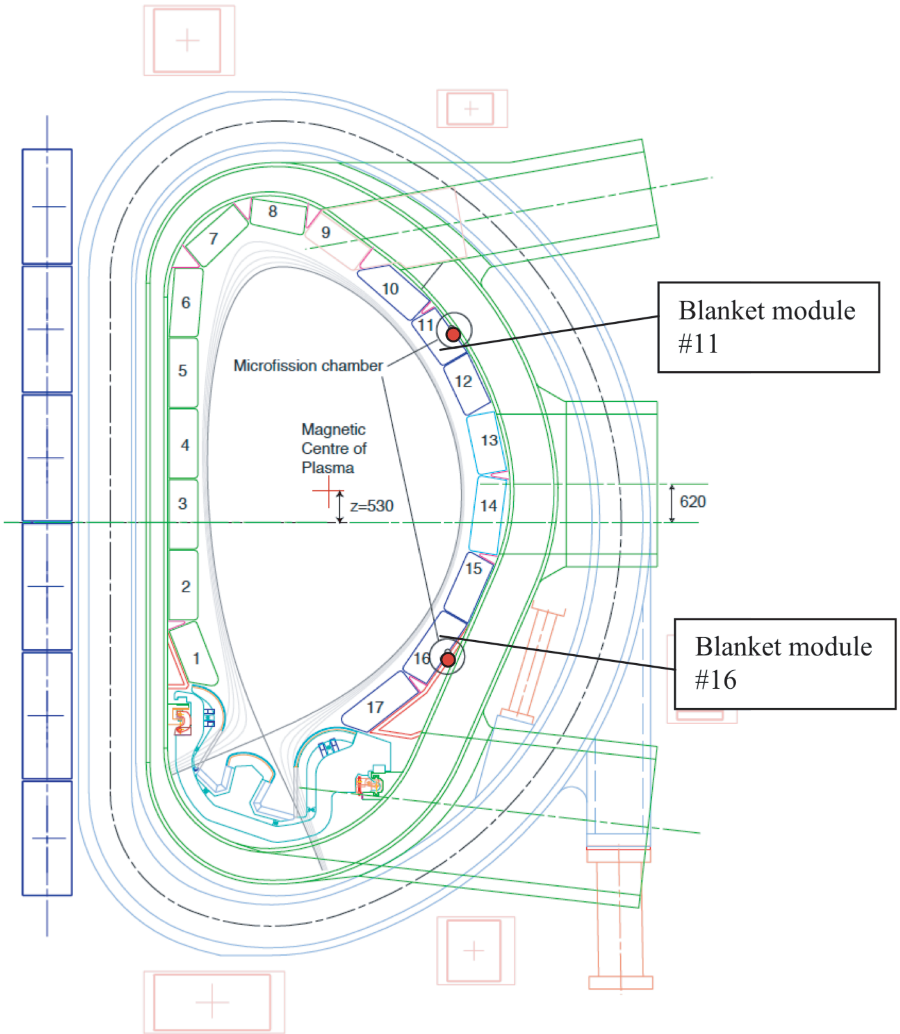

Fig.2-2-1

Arrangement of the MFC on the poloidal cross-section of ITER

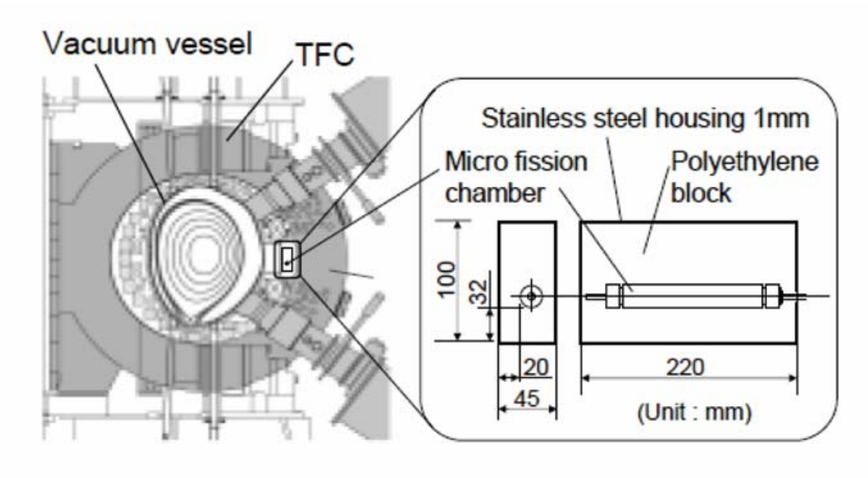

Fig.2.4-1
Location of the MFC on the poloidal cross-section of JT-60U

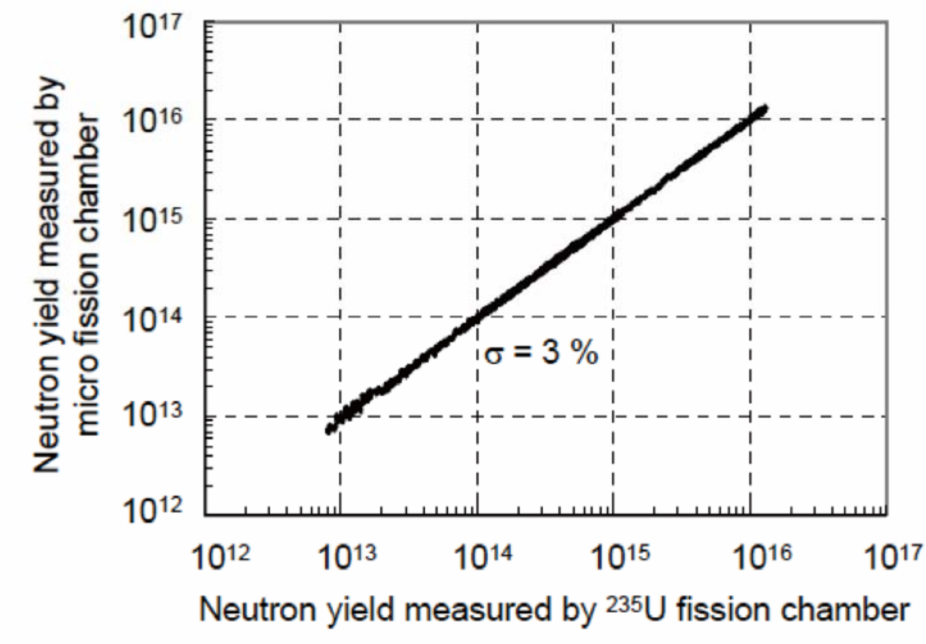

Fig.2.4-2
Linearity between the MFC and the neutron monitor of JT-60U

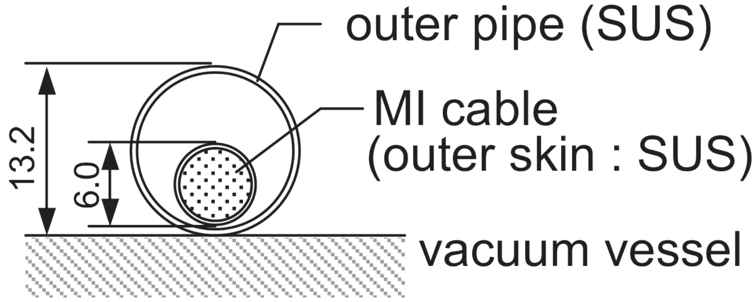

Fig. 3.1-1
Schematic of the double pipe structure

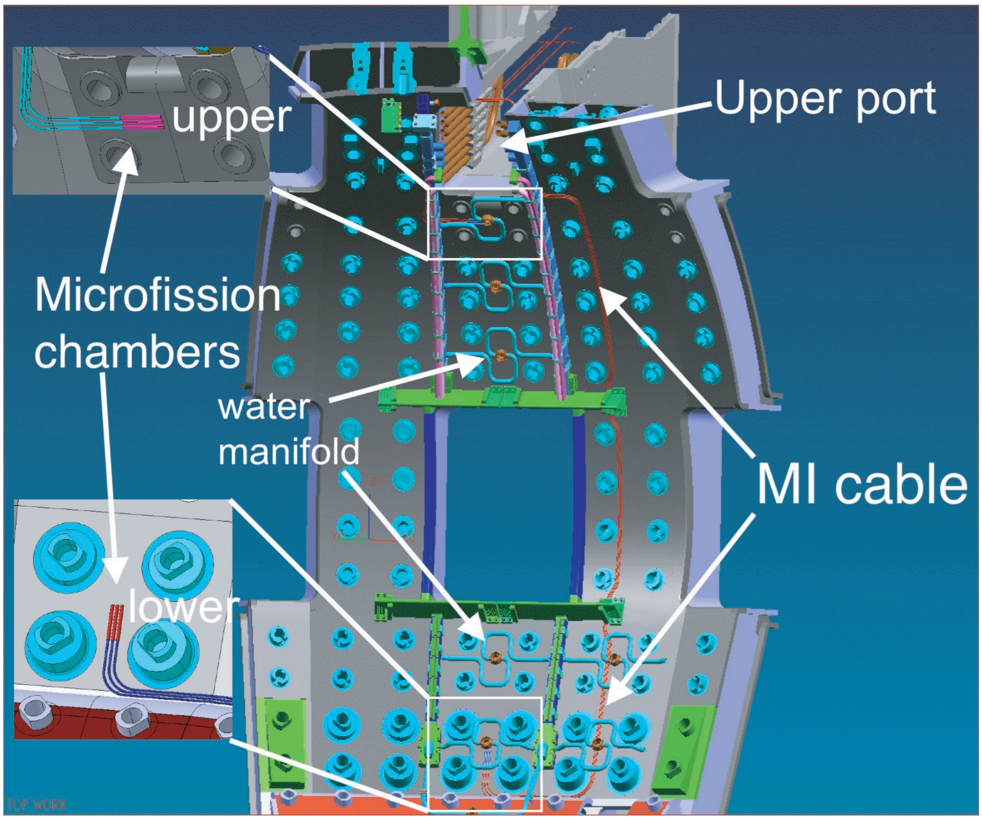

Fig.3.2-1

Whole cable route of the MI cable of MFCs on the vacuum vessel

This is a blank page.

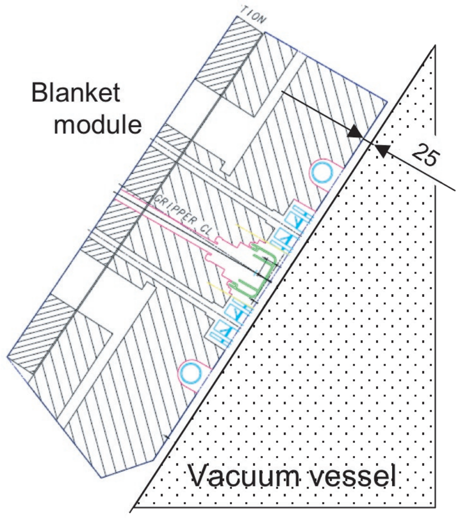

Fig.3.2-2
Schematic view of the vacuum vessel and the blanket module

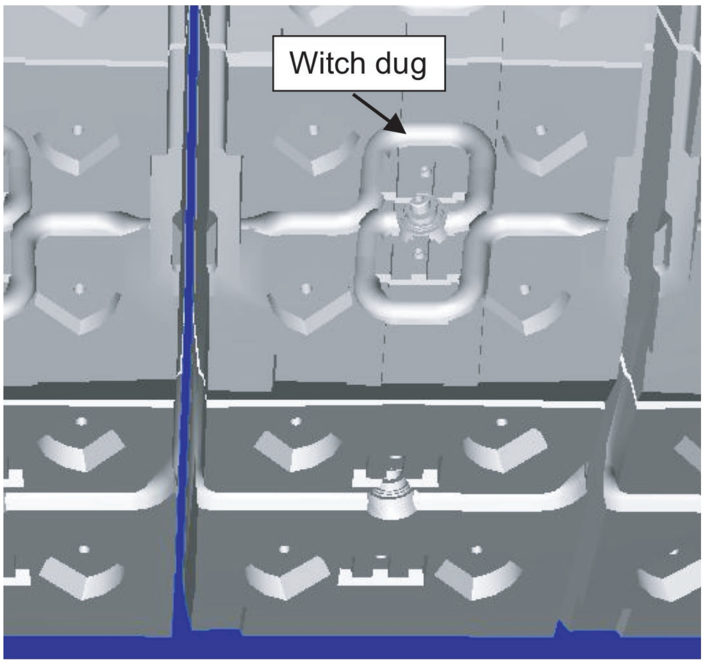

Fig.3.2-3
Expanded view of rear of the blanket module

This is a blank page.

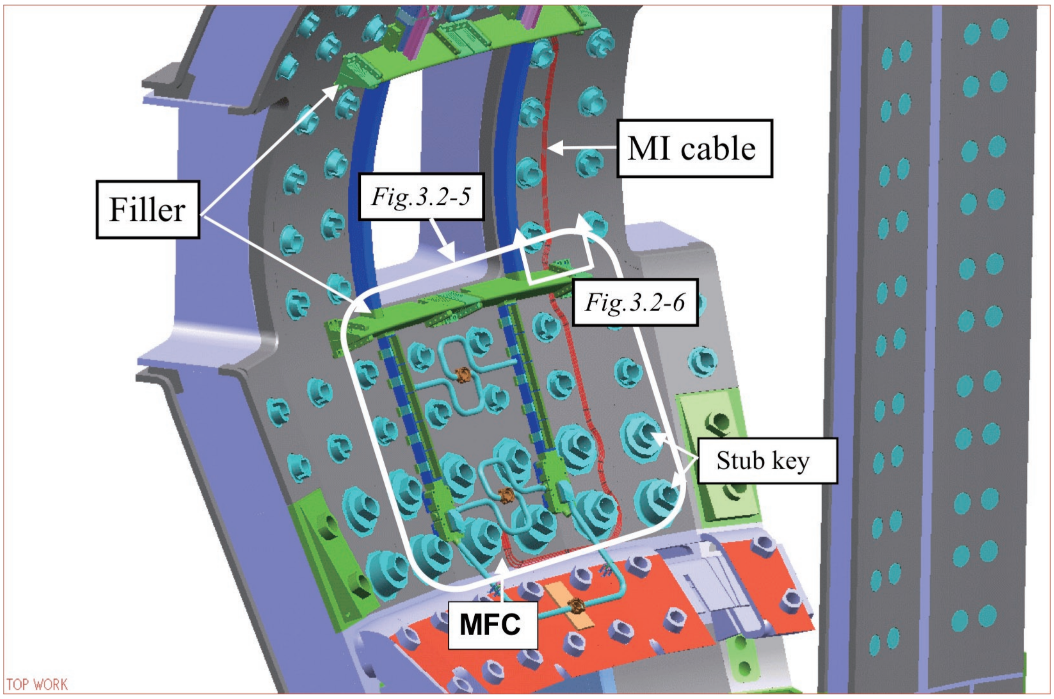

Fig. 3.2-4
Cable route of the MI cable of the lower MFC on the vacuum vessel

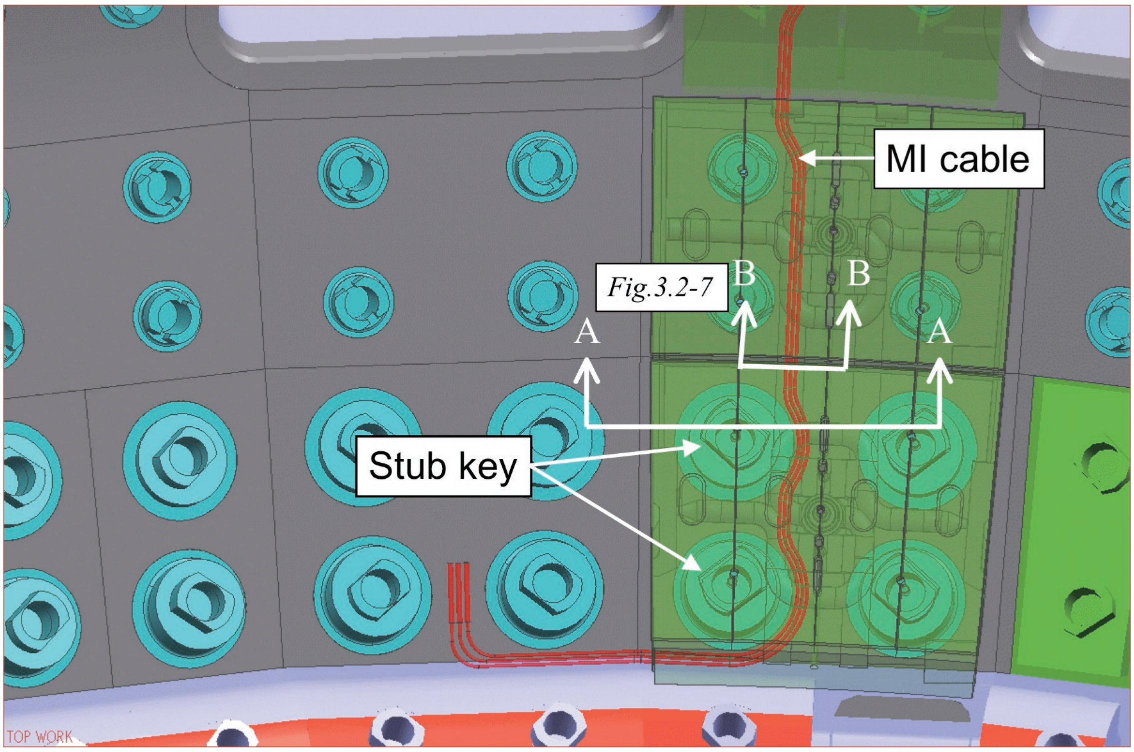

Fig.3.2-5

Expanded view of cable route of the MI cable of the lower MFC near the stub key on the lower vacuum vessel

This is a blank page.

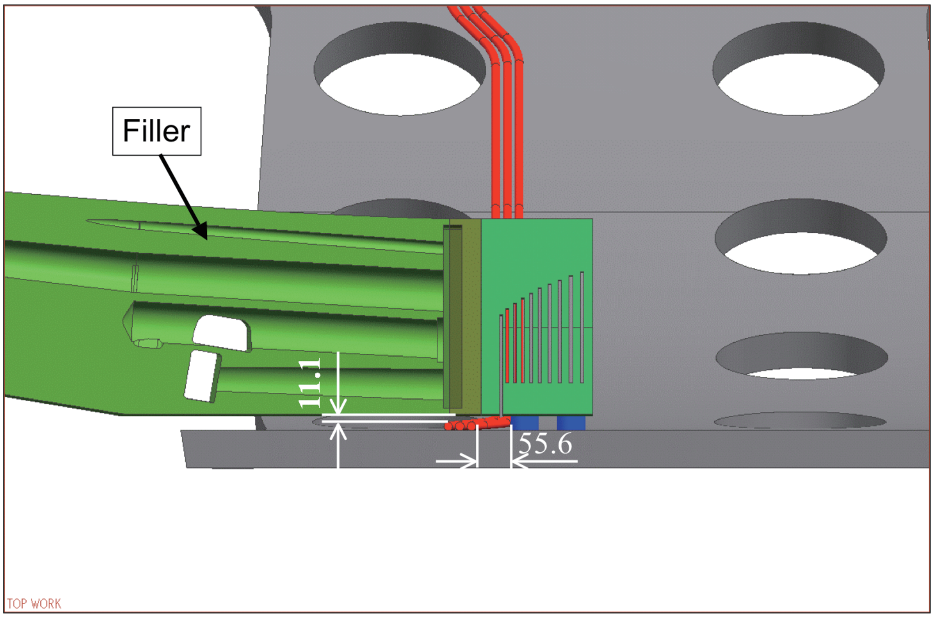

Fig.3.2-6

Cross sectional view of cable route under the filler

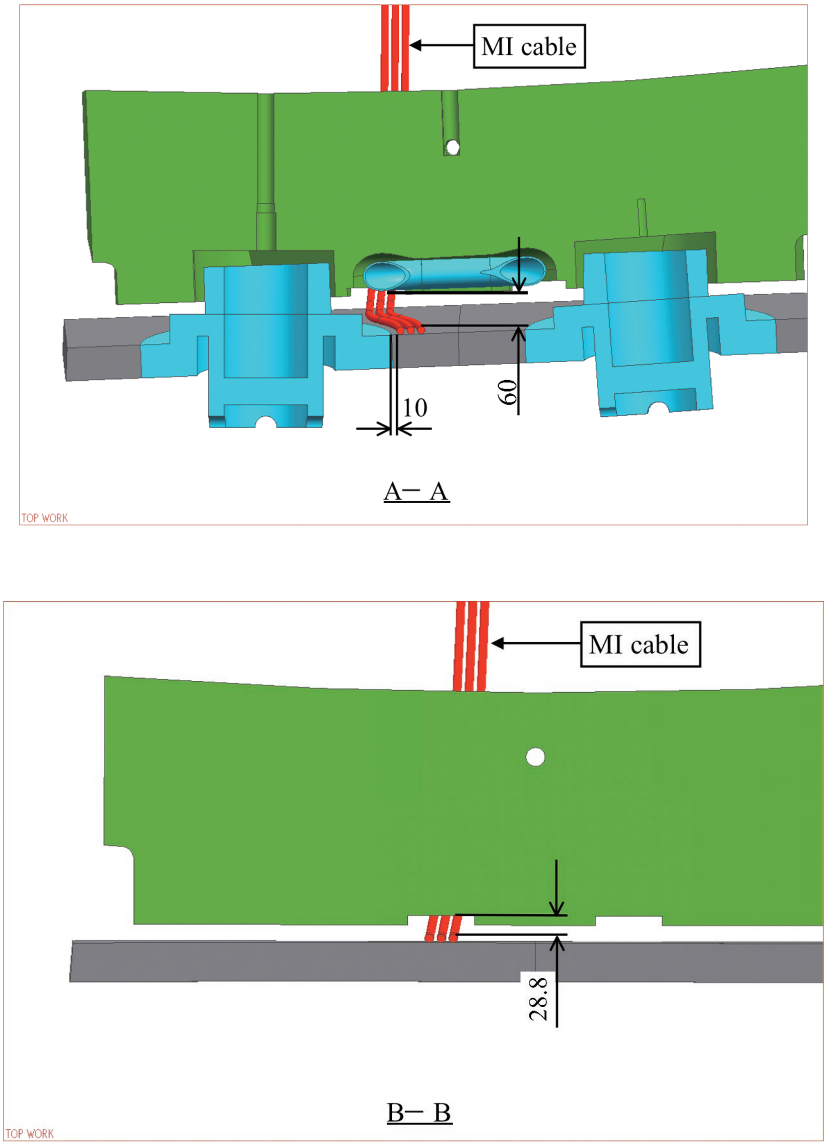

Fig.3.2-7
Cross sectional view of cable route under the blanket module

This is a blank page.

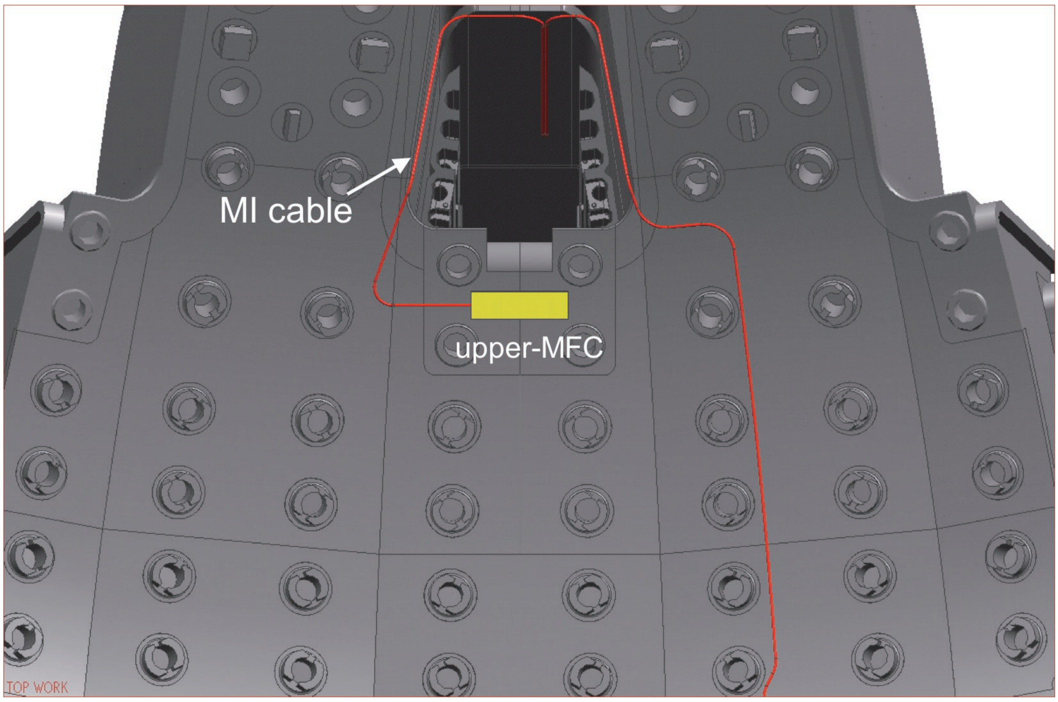

Fig.3.2-8
Cable route of the MI cable for the upper-MFC on the vacuum vessel

This is a blank page.

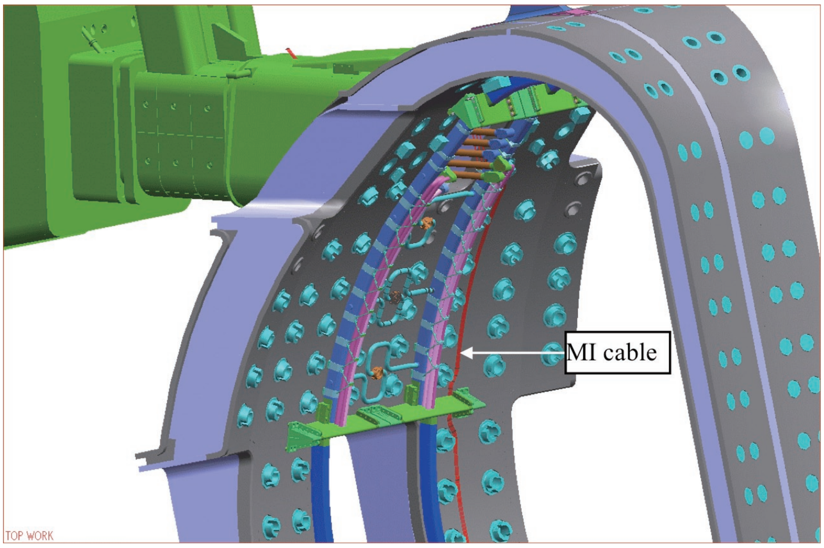

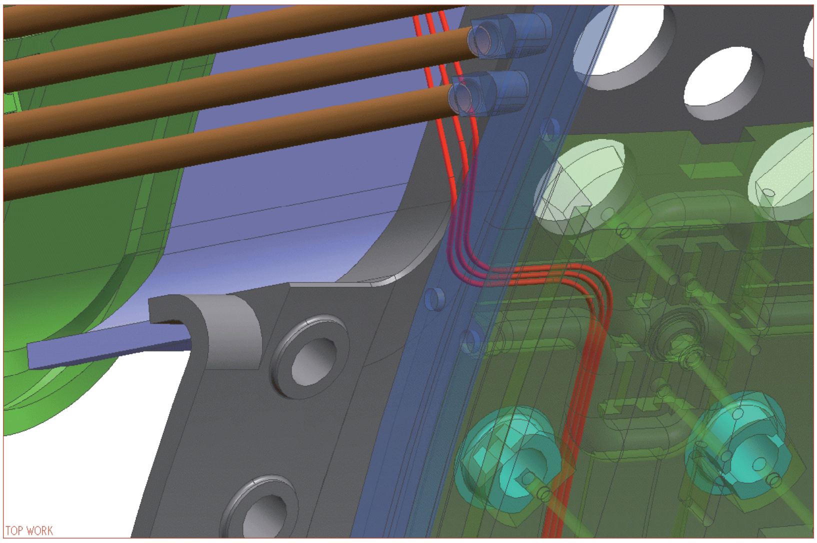

Fig.3.2-9

Cable route near the upper port of the MI cable of the lower-MFC

This is a blank page.

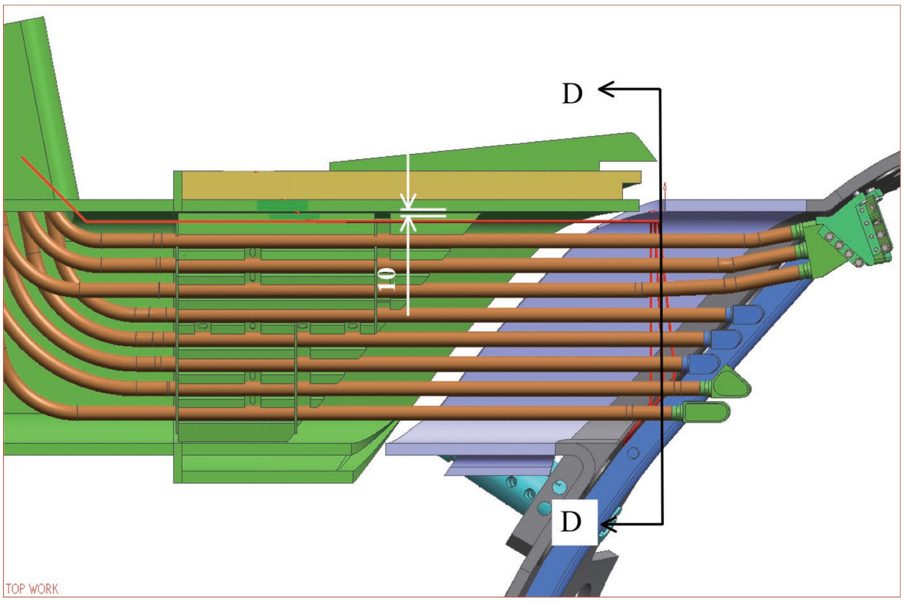

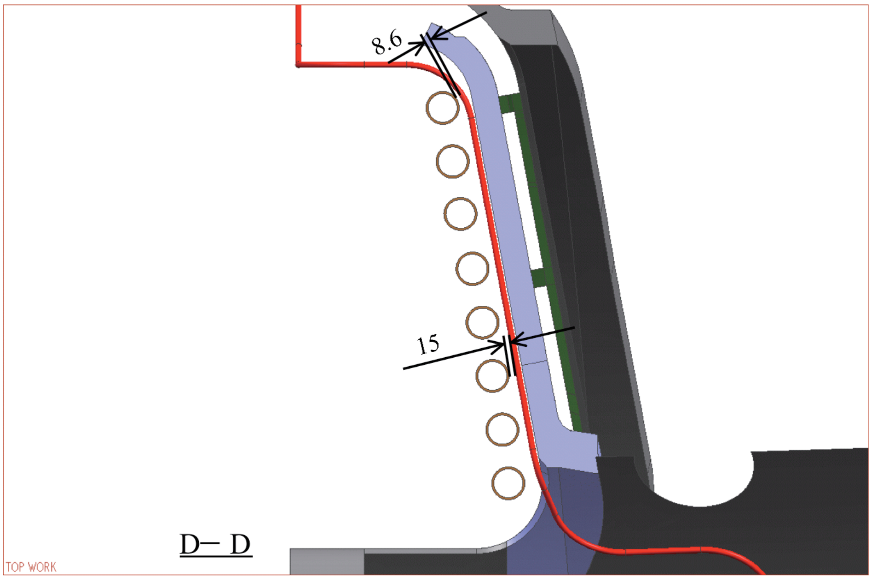

Fig.3.2-10

Cable route of the MI cable of the lower-MFC in the upper port

This is a blank page.

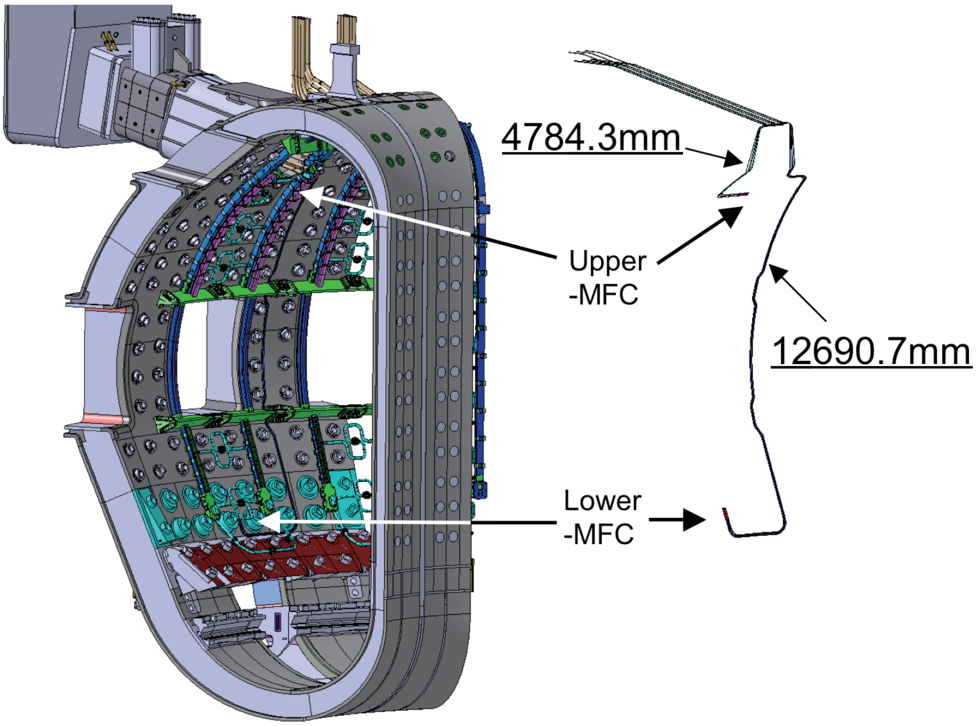

(a) (b)

Fig.3.3-1
Whole cable rout of the MI cable

This is a blank page.

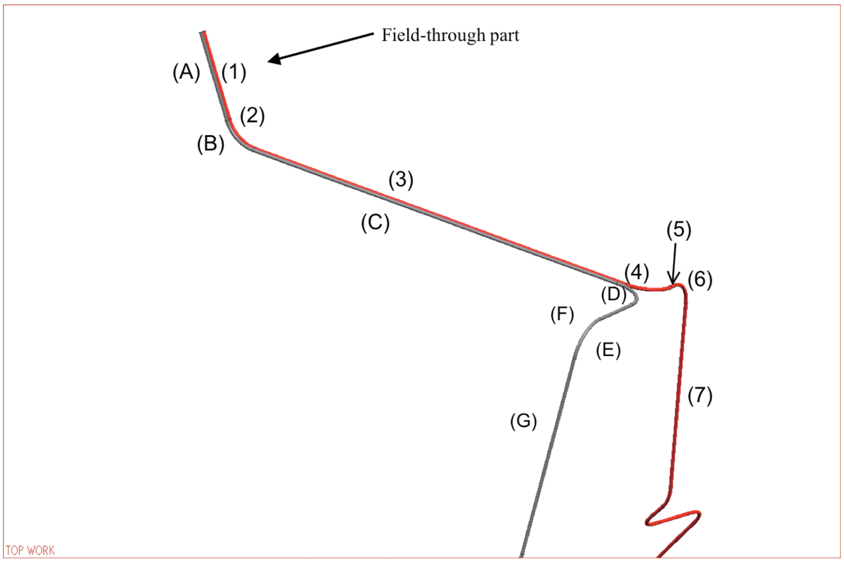

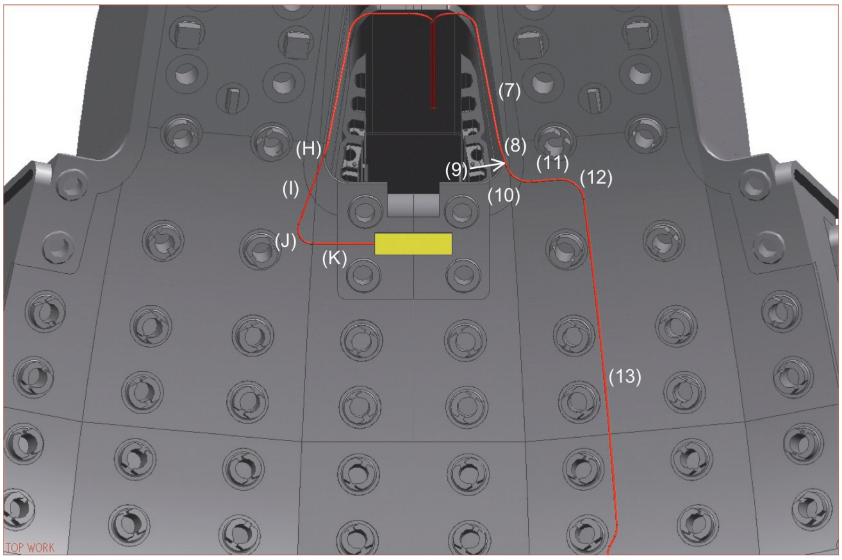

Fig.3.3-2

Schematic view of bending point of the MI cable in and near the upper port

This is a blank page.

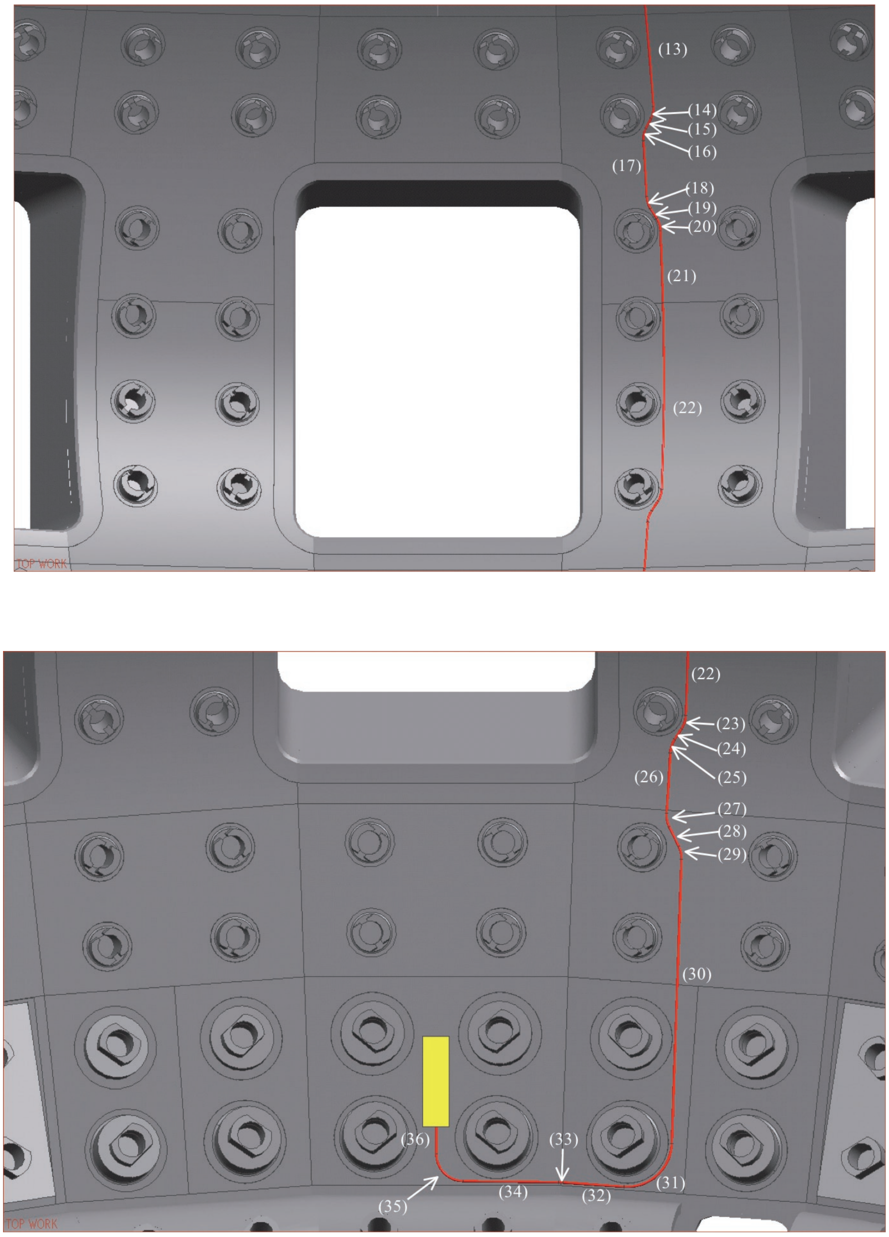

Fig.3.3-3

Schematic view of bending point of the MI cable for lower-MFC on the vacuum vessel

This is a blank page.

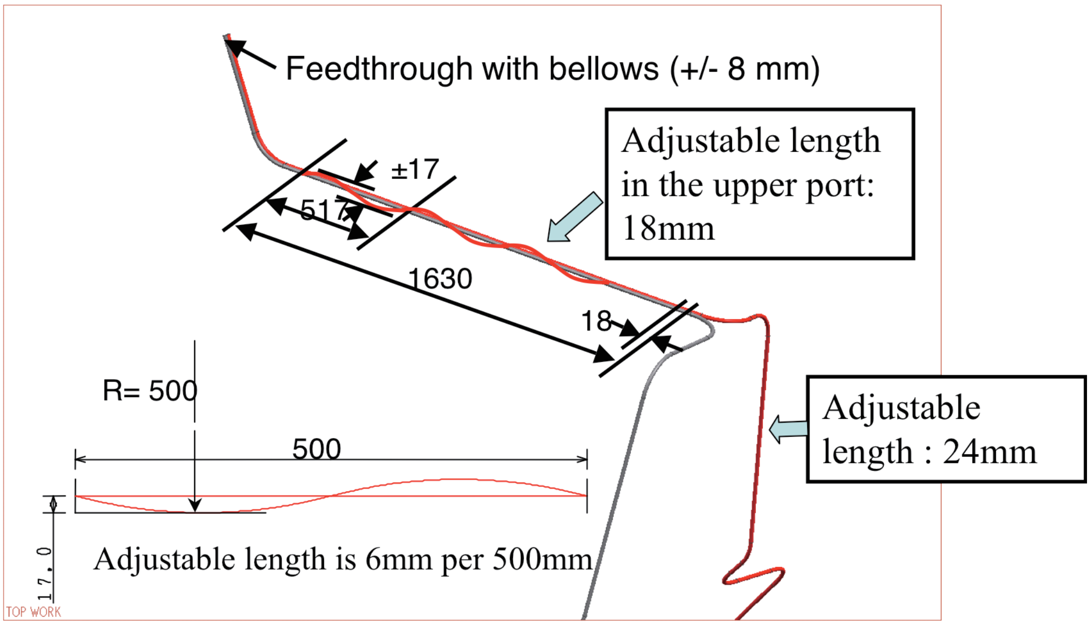

Fig.3.4-1
Adjust of length of the MI cable

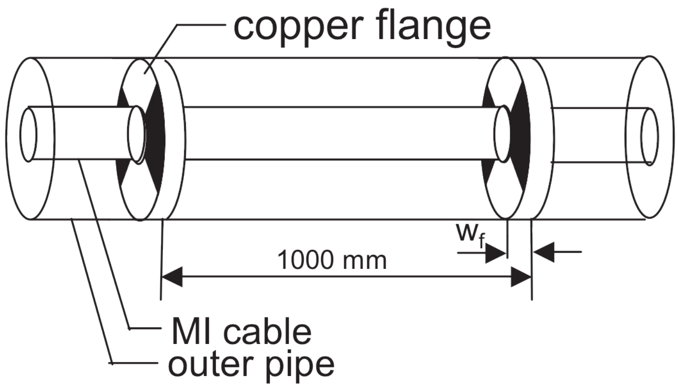

Fig. 3.5-1

Conceptual structure of the double pipe for suppression of temperature rise of the MI cable

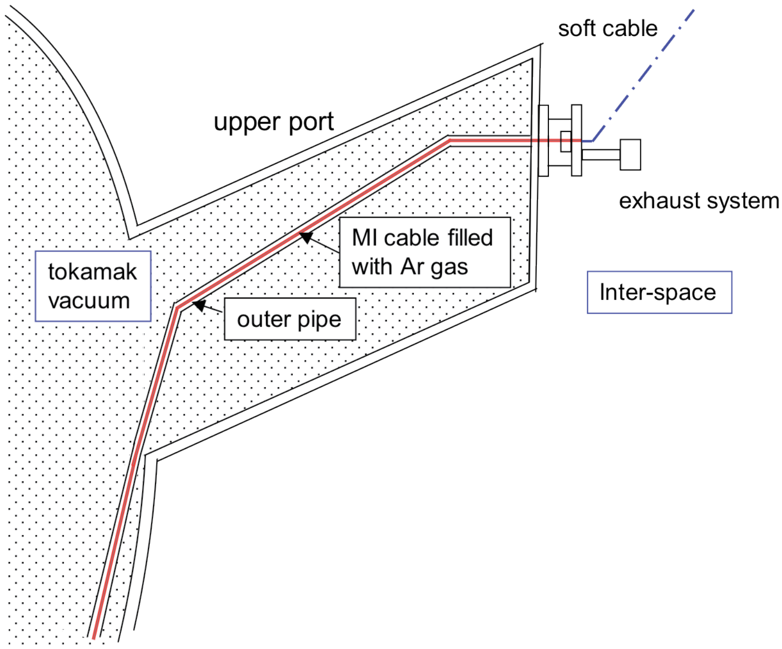

Fig.4.1-1

Constructive concept of the terminal of the double pipe

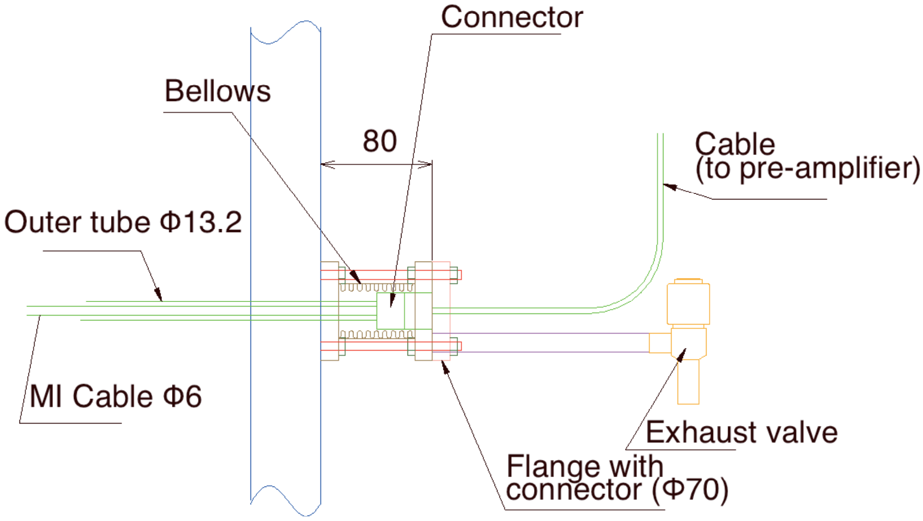

Fig.4.2-1

Schematic view of the structure of the feed-through

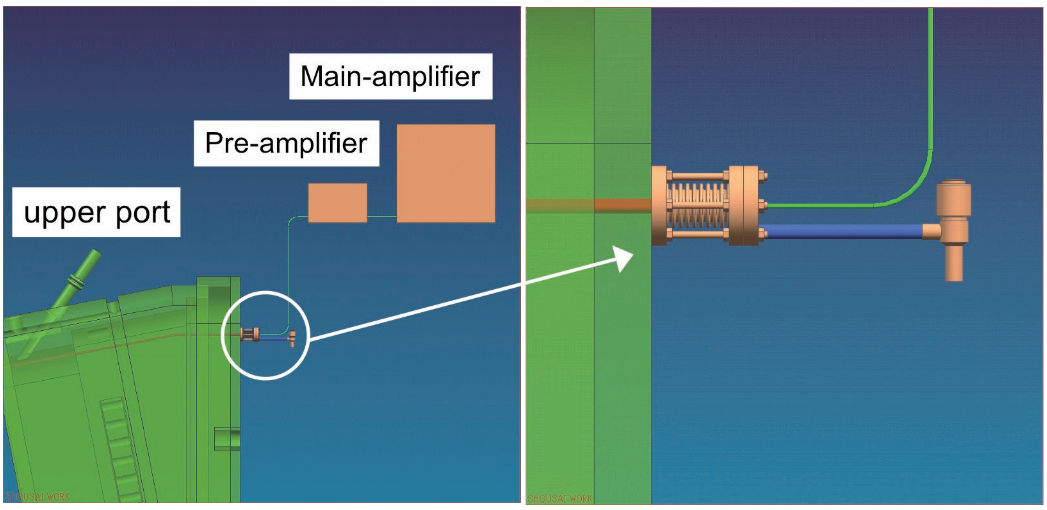

Fig.4.2-2

Schematic view around the feed-through

国際単位系（SI）

表１．SI 基本単位

基本量	SI 基本単位	
	名称	記号
長さ	メートル	m
質量	キログラム	kg
時間	秒	s
電流	アンペア	A
熱力学温度	ケルビン	K
物質量	モル	mol
光度	カンデラ	cd

表２．基本単位を用いて表されるSI組立単位の例

組立量	SI 基本単位	
	名称	記号
面積	平方メートル	m^2
体積	立法メートル	m^3
速さ，速度	メートル毎秒	m/s
加速度	メートル毎秒毎秒	m/s^2
波数	毎メートル	m-1
密度（質量密度）	キログラム毎立法メートル	kg/m^3
質量体積（比体積）	立法メートル毎キログラム	m^3/kg
電流密度	アンペア毎平方メートル	A/m^2
磁界の強さ	アンペア毎メートル	A/m
（物質量の）濃度	モル毎立方メートル	mol/m^3
輝度	カンデラ毎平方メートル	cd/m^2
屈折率	（数の）　１	1

表５．SI 接頭語

乗数	接頭語	記号	乗数	接頭語	記号
10^{24}	ヨタ	Y	10^{-1}	デシ	d
10^{21}	ゼタ	Z	10^{-2}	センチ	c
10^{18}	エクサ	E	10^{-3}	ミリ	m
10^{15}	ペタ	P	10^{-6}	マイクロ	μ
10^{12}	テラ	T	10^{-9}	ナノ	n
10^{9}	ギガ	G	10^{-12}	ピコ	p
10^{6}	メガ	M	10^{-15}	フェムト	f
10^{3}	キロ	k	10^{-18}	アト	a
10^{2}	ヘクト	h	10^{-21}	ゼプト	z
10^{1}	デカ	da	10^{-24}	ヨクト	y

表３．固有の名称とその独自の記号で表されるSI組立単位

組立量	SI 組立単位			
	名称	記号	他のSI単位による表し方	SI基本単位による表し方
平面角	ラジアン[a]	rad		m・m^{-1}=1[b]
立体角	ステラジアン[a]	sr[c]		m^2・m^{-2}=1[b]
周波数	ヘルツ	Hz		s^{-1}
力	ニュートン	N		m・kg・s^{-2}
圧力，応力	パスカル	Pa	N/m^2	m^{-1}・kg・s^{-2}
エネルギー，仕事，熱量	ジュール	J	N・m	m^2・kg・s^{-2}
工率，放射束	ワット	W	J/s	m^2・kg・s^{-3}
電荷，電気量	クーロン	C		s・A
電位差（電圧），起電力	ボルト	V	W/A	m^2・kg・s^{-3}・A^{-1}
静電容量	ファラド	F	C/V	m^{-2}・kg^{-1}・s^4・A^2
電気抵抗	オーム	Ω	V/A	m^2・kg・s^{-3}・A^{-2}
コンダクタンス	ジーメンス	S	A/V	m^{-2}・kg^{-1}・s^3・A^2
磁束	ウエーバ	Wb	V・s	m^2・kg・s^{-2}・A^{-1}
磁束密度	テスラ	T	Wb/m^2	kg・s^{-2}・A^{-1}
インダクタンス	ヘンリー	H	Wb/A	m^2・kg・s^{-2}・A^{-2}
セルシウス温度	セルシウス度[d]	℃		K
光束	ルーメン	lm	cd・sr[c]	m^2・m^{-2}・cd=cd
照度	ルクス	lx	lm/m^2	m^2・m^{-4}・cd=m^{-2}・cd
（放射性核種の）放射能	ベクレル	Bq		s^{-1}
吸収線量，質量エネルギー分与，カーマ	グレイ	Gy	J/kg	m^2・s^{-2}
線量当量，周辺線量当量，方向性線量当量，個人線量当量，組織線量当	シーベルト	Sv	J/kg	m^2・s^{-2}

(a) ラジアン及びステラジアンの使用は、同じ次元であっても異なった性質をもった量を区別するときの組立単位の表し方として利点がある。組立単位を形作るときのいくつかの用例は表４に示されている。
(b) 実際には、使用する時には記号rad及びsrが用いられるが、習慣として組立単位としての記号“１”は明示されない。
(c) 測光学では、ステラジアンの名称と記号srを単位の表し方の中にそのまま維持している。
(d) この単位は、例としてミリセルシウス度m℃のようにSI接頭語を伴って用いても良い。

表４．単位の中に固有の名称とその独自の記号を含むSI組立単位の例

組立量	SI 組立単位		
	名称	記号	SI 基本単位による表し方
粘度	パスカル秒	Pa・s	m^{-1}・kg・s^{-1}
力のモーメント	ニュートンメートル	N・m	m^2・kg・s^{-2}
表面張力	ニュートン毎メートル	N/m	kg・s^{-2}
角速度	ラジアン毎秒	rad/s	m・m^{-1}・s^{-1}=s^{-1}
角加速度	ラジアン毎平方秒	rad/s^2	m・m^{-1}・s^{-2}=s^{-2}
熱流密度，放射照度	ワット毎平方メートル	W/m^2	kg・s^{-3}
熱容量，エントロピー	ジュール毎ケルビン	J/K	m^2・kg・s^{-2}・K^{-1}
質量熱容量（比熱容量），質量エントロピー	ジュール毎キログラム毎ケルビン	J/(kg・K)	m^2・s^{-2}・K^{-1}
質量エネルギー（比エネルギー）	ジュール毎キログラム	J/kg	m^2・s^{-2}・K^{-1}
熱伝導率	ワット毎メートル毎ケルビン	W/(m・K)	m・kg・s^{-3}・K^{-1}
体積エネルギー	ジュール毎立方メートル	J/m^3	m^{-1}・kg・s^{-2}
電界の強さ	ボルト毎メートル	V/m	m・kg・s^{-3}・A^{-1}
体積電荷	クーロン毎立方メートル	C/m^3	m^{-3}・s・A
電気変位	クーロン毎平方メートル	C/m^2	m^{-2}・s・A
誘電率	ファラド毎メートル	F/m	m^{-3}・kg^{-1}・s^4・A^2
透磁率	ヘンリー毎メートル	H/m	m・kg・s^{-2}・A^{-2}
モルエネルギー	ジュール毎モル	J/mol	m^2・kg・s^{-2}・mol^{-1}
モルエントロピー，モル熱容量	ジュール毎モル毎ケルビン	J/(mol・K)	m^2・kg・s^{-2}・K^{-1}・mol^{-1}
照射線量（Ｘ線及びγ線）	クーロン毎キログラム	C/kg	kg^{-1}・s・A
吸収線量率	グレイ毎秒	Gy/s	m^2・s^{-3}
放射強度	ワット毎ステラジアン	W/sr	m^4・m^{-2}・kg・s^{-3}=m^2・kg・s^{-3}
放射輝度	ワット毎平方メートル毎ステラジアン	W/(m^2・sr)	m^2・m^{-2}・kg・s^{-3}=kg・s^{-3}

表６．国際単位系と併用されるが国際単位系に属さない単位

名称	記号	SI 単位による値
分	min	1 min=60s
時	h	1h =60 min=3600 s
日	d	1 d=24 h=86400 s
度	°	1° =(π/180) rad
分	′	1′ =(1/60)° =(π/10800) rad
秒	″	1″ =(1/60)′ =(π/648000) rad
リットル	l、L	1l=1 dm^3=10^{-3}m^3
トン	t	1t=10^3 kg
ネーパ	Np	1Np=1
ベル	B	1B=(1/2)ln10(Np)

表７．国際単位系と併用されこれに属さない単位でSI単位で表される数値が実験的に得られるもの

名称	記号	SI 単位であらわされる数値
電子ボルト	eV	1eV=1.60217733(49)×10^{-19}J
統一原子質量単位	u	1u=1.6605402(10)×10^{-27}kg
天文単位	ua	1ua=1.49597870691(30)×10^{11}m

表８．国際単位系に属さないが国際単位系と併用されるその他の単位

名称	記号	SI 単位であらわされる数値
海里		1海里=1852m
ノット		1ノット=1海里毎時=(1852/3600)m/s
アール	a	1 a=1 dam^2=10^{2}m^2
ヘクタール	ha	1 ha=1 hm^2=10^{4}m^2
バール	bar	1 bar=0.1MPa=100kPa=1000hPa=10^{5}Pa
オングストローム	Å	1 Å=0.1nm=10^{-10}m
バーン	b	1 b=100fm^2=10^{-28}m^2

表９．固有の名称を含むCGS組立単位

名称	記号	SI 単位であらわされる数値
エルグ	erg	1 erg=10^{-7} J
ダイン	dyn	1 dyn=10^{-5}N
ポアズ	P	1 P=1 dyn・s/cm^2=0.1Pa・s
ストークス	St	1 St =1cm^2/s=10^{-4}m^2/s
ガウス	G	1 G ˆ10^{-4}T
エルステッド	Oe	1 Oe ˆ(1000/4π)A/m
マクスウェル	Mx	1 Mx ˆ10^{-8}Wb
スチルブ	sb	1 sb =1cd/cm^2=10^{4}cd/m^2
ホト	ph	1 ph=10^{4}lx
ガル	Gal	1 Gal =1cm/s^2=10^{-2}m/s^2

表10．国際単位に属さないその他の単位の例

名称	記号	SI 単位であらわされる数値
キュリー	Ci	1 Ci=3.7×10^{10}Bq
レントゲン	R	1 R = 2.58×10^{-4}C/kg
ラド	rad	1 rad=1cGy=10^{-2}Gy
レム	rem	1 rem=1 cSv=10^{-2}Sv
X線単位		1X unit=1.002×10^{-4}nm
ガンマ	γ	1γ=1 nT=10^{-9}T
ジャンスキー	Jy	1 Jy=10^{-26}W・m^{-2}・Hz^{-1}
フェルミ		1 fermi=1 fm=10^{-15}m
メートル系カラット		1 metric carat = 200 mg = 2×10^{-4}kg
トル	Torr	1 Torr = (101 325/760) Pa
標準大気圧	atm	1 atm = 101 325 Pa
カロリー	cal	
ミクロン	μ	1 μ =1μm=10^{-6}m

（第７版，1998年改訂）